Published in final edited form as:
Cell Immunol. 2007 ; 250(1-2): 40–54.

Quantitative analysis of T Cell Homeostatic Proliferation

Cheng-Rui Li[a,b], **Sharon Santoso**[b,c], and **David D. Lo**[a,b*]

a*Division of Biomedical Sciences, University of California Riverside, Riverside, CA 92521, USA and Division of Developmental Immunology*

b*La Jolla Institute for Allergy and Immunology, 9420 Athena Circle, La Jolla, CA 92037, USA*

c*University of California, San Diego, La Jolla, CA 92037, USA*

Abstract

T cell homeostatic proliferation occurs on transfer of T cells into lymphopenic recipients; transferred cells undergo several rounds of division in the absence of specific antigen stimulation. For a quantitative analysis of this phenomenon, we applied a mathematical method to describe proliferating T cells to match peak distributions from actual CFSE dilution data. For *in vitro* stimulation of T cells with anti-CD3/anti-CD28, our simulation confirmed a high proportion of cells entering cell cycle with a low proportion undergoing apoptosis. When applied to homeostatic proliferation, it described striking differences in CD4 and CD8 T cell proliferation rates, and accurately predicted that successive divisions were accompanied by higher rates of apoptosis, limiting the accumulation of proliferating cells. Thus, the presence of multiple CFSE dilution peaks cannot be considered equivalent to lymphocyte expansion. Finally, genetic effects were identified that may help explain links between homeostatic proliferation and autoimmunity.

Keywords

Homeostatic proliferation; $CD4^+$ T cell; $CD8^+$ T cell; Modeling

Introduction

In humans and animals, there are thought to be homeostatic mechanisms that attempt to keep T cell numbers at relatively stable levels [1]. Thus, when the T cell population is seriously depleted, the remaining T cells undergo proliferation. This has been referred to as T cell homeostatic proliferation, or lymphopenia induced proliferation [2]. It is generally accepted that although T cell homeostatic proliferation does not depend on stimulation by a high affinity target antigen, it still requires recognition of MHC plus self peptide by TCR [3,4,5,6]. In addition, some common γ chain (γ_C) cytokines, especially IL-7, support this process [7,8]. Despite the absence of antigen stimulation, naïve T cells can acquire a memory phenotype and function after homeostatic proliferation [6,9,10]. Furthermore, these cells may contribute to the induction or precipitation of autoimmune diseases [11,12,13]. However, detailed molecular mechanisms that initiate and control T cell homeostatic proliferation have not been fully elucidated.

*Correspondence should be addressed to Dr. David D. Lo, Division of Biomedical Sciences, University of California Riverside, 900 University Ave., Riverside, CA 92521, USA, Phone: +1-951-827-4553, Fax: +1-951-827-5504, E-mail: <david.lo@ucr.edu>.

Conflict of interest The authors declare that they have no financial conflict of interest.

In experiments studying T cell homeostatic proliferation, a widely used method is adoptive transfer of carboxy-fluorescein-diacetate succinimidylester (CFSE)-loaded T cells into T cell-depleted mice, and assessing division of transferred T cells by CFSE dilution [14,15]. This method provides a convenient means to analyze cell division, so most previous studies focused only on factors controlling the presence or absence of proliferation [15]. However, the accumulated T cell pool remaining after homeostatic proliferation is determined not only by proliferation itself, but also by the survival of extant cells.

Previous studies on homeostatic proliferation only described CFSE dilution qualitatively without any quantitation of the CFSE dilution profiles. This is despite several recent studies [16–24] using the ability of CFSE to mark dividing cell populations to develop various mathematical analyses of cell proliferation dynamics. In these reports, mathematical methods were applied to quantify components of T cell responses such as cell generation times and proliferative capacity, though they were most often used only to study in vitro response to cytokines or antibodies. They have not yet been used to characterize how varying extrinsic and intrinsic factors might be responsible for differences T cell proliferation in situations such as homeostatic proliferation; it is possible that the complexity of the analytical approaches used made it difficult to apply routinely in common cellular immune systems in vivo.

Yet since CFSE dilution data is clearly amenable to mathematical analysis, we sought to carefully quantify homeostatic T cell proliferation, but using a simpler mathematical approach considering only a few parameters, such as cell division and survival/cell-death. We also validated this system in controlled *in vitro* T cell proliferation assays. Importantly, the results of this approach lead to interesting predictions which were experimentally confirmed. Using this modeling system, we provide clues to the strikingly different rates of homeostatic proliferation of $CD4^+$ versus $CD8^+$ T cells, and interestingly, we were able to identify some genetic background effects on T cell homeostatic proliferation. Such information may provide important insights to the major differences in the regulation of T cell subset biology, and genetic factors that may influence T cell effector responses, including susceptibility to immunologically mediated diseases.

Results

$CD4^+$ and $CD8^+$ T cells proliferate with different kinetics under lymphopenic or TCR-activated conditions

Many previous studies investigated homeostatic proliferation on $CD4^+$ or $CD8^+$ T cells separately, using transgenic TCR expressing T cells [4,5,9,25,26]. We were interested in investigating T cell homeostatic proliferation within both $CD4^+$ and $CD8^+$ T cell subsets. We first purified total T cells from normal BALB/c mice, loaded them with CFSE, and adoptively transferred into sub-lethally irradiated BALB/c mice. Seven and fourteen days after transfer, lymph node (LN) cells and splenocytes (SP) from the transferred mice were harvested and analyzed. The proliferation kinetics, as shown by CFSE dilution profiles, was strikingly different between $CD4^+$ and $CD8^+$ T cells (Figure 1A). For the $CD4^+$ T cell subset, seven days after transfer, the majority of the transferred cells remained undivided, and a small proportion of cells divided beyond three generations. Even two weeks after transfer, only a small percentage of $CD4^+$ T cells divided more than three times, while most cells stopped at the first generation of division. In contrast, the co-transferred $CD8^+$ T cells divided more extensively than $CD4^+$ T cells. Seven days after transfer, a significant percentage of $CD8^+$ T cells had divided more than six times; at the day fourteen time point, some cells had divided beyond CFSE detection limit (Figure 1A and data not shown). These data would appear to suggest that, in lymphopenic environments, $CD8^+$ T cells proliferate more rapidly than $CD4^+$ T cells.

To compare T cell behaviors between homeostatic proliferation and TCR/costimulation triggered proliferation, CFSE-loaded total T cells were analyzed for proliferation in response to anti-CD3 alone versus anti-CD3 plus anti-CD28 costimulation [27]. As expected, anti-CD3 plus anti-CD28 costimulation activated more T cells, both $CD4^+$ and $CD8^+$, and to a larger extent compared to anti-CD3 alone (Figure 1B). As with lymphopenia induced homeostatic proliferation, clear differences also can be seen between $CD4^+$ and $CD8^+$ subsets. For instance, upon either anti-CD3 alone stimulation or anti-CD3 plus anti-CD28 costimulation, a smaller proportion of $CD4^+$ T cells was left undivided after three days compared to $CD8^+$ T cells. Furthermore, the CFSE dilution profiles showed striking differences in T cell proliferation kinetics upon different induction conditions (Figure 1).

Quantitation of CFSE profiles and mathematical simulation: selection of parameters

Tracking CFSE dilution in adoptive transfer experiments has been a widely used method in studying T cell homeostatic proliferation [14,15]. However, there are no studies on homeostatic proliferation of T cell subsets in vivo that have used CFSE data to identify factors accounting for cell accumulation or relative proliferation rates. Therefore, we decided to apply a simple analysis on the CFSE profiles to establish quantitative characteristics of proliferation that would enable comparisons among cell types and experimental conditions. To this end, we first calculated the percentage of each CFSE peak amongst the whole CFSE positive population, as shown in Figure 1.

With CFSE peak data, what would be the best parameters to consider for our mathematical analysis? Several recent studies have been presented [16–24] using mathematical modeling approaches to analyze CFSE-labeled T cell proliferation; while there was considerable variation in experimental and analytical approach, they can provide some guidance four our study. In studies focusing on the regulation of cell cycle [19–24], the main factors included in the mathematical analysis include the proportion of cells entering cell cycle, and the time occupied in cell cycle, including transition periods prior to entry into cell cycle. In the most detailed analyses, the focus has been on identifying the discrete events regulating cell division, and interestingly, in some cases the time within the cell cycle appeared to be relatively constant [17,19,22,23], though not always [24]. One aspect that remains resistant to analysis is the apparent variation in time between initial stimulation of the culture and entry of individual cells into cell cycle. That is, the population was not synchronized in its response to stimulation, consistent with stochastic aspects of commitment to proliferate [19–24]. Therefore, from the point of view of identifying quantitative characters for comparing cells and conditions, we prefer the simplification of assuming a constant time per cell cycle, and collapsing the random time of entry to cell cycle by establishing a factor defining the proportion of cells entering cell cycle during any discrete period (defined as an arbitrary “cycle” in our method).

More general parameters have also been included in some modeling studies, such as mean cell division number for the whole population [19,23], the total number of mitotic events [16], and proliferative capacity of cells committed to proliferation after initial stimulation [16,17]. Such calculated parameters may help characterize the population, but may be too many steps removed from cell intrinsic or environmental factors to provide useful direct comparisons among experiments.

Another important parameter would be the loss of cells over time or at each cell division due to apoptosis or other mode of exit, but curiously, in some of the studies this was not taken into account [16,17]. While dead CFSE positive cells may persist in vitro for a few days [16], apoptosis of cells and their subsequent disposal would be an important factor in cell division and accumulation [18,19] especially in vivo. Physiological changes (e.g., differentiation) in T cells in response to stimulation should have an influence on the proportion of cells lost to apoptosis or other mechanism at each cell division. This was briefly considered in one

discussion in a "heterogeneous model" [23], and incremental increases in apoptosis rates at each cell division were found to be a critical characteristic in the response to superantigen stimulation [18]. Unfortunately, all other approaches kept the rate of cell loss as a constant factor at each cell division; this might be an inappropriate simplification of T cell responses.

This notion of physiological changes or differentiation in response to stimulation should apply to both the proportion of cells entering cell cycle at each cell division, and the proportion of cells lost to apoptosis. Since our interest is in the effects of homeostatic proliferation on both differentiation and cell loss, we have chosen to include the possibility for incrementally changing proportions at each cell division. Thus, while some other approaches have gone to greater lengths to incorporate factors such as time in cell cycle, we have instead attended to the potential for changes at each successive cell division; the distribution of cells among CFSE peaks may be a direct clue to such effects.

A technical consideration for *in vivo* homeostatically proliferating T cells is that migration from lymphoid organs to peripheral non-lymphoid organs could also affect detection of labeled cells. However, when we analyzed the lung as an example of non-lymphoid organs, we did not find differences in the percentages of T cells and T cell subsets in the lungs from normal, irradiated but not transferred (Irr-N), and irradiated and transferred (Irr) mice (not shown). This suggests that migration to non-lymphoid organs would not be a major outcome for homeostatically proliferating T cells in hosts that are not infected with specific pathogens. In any case, cells lost from the recirculating lymphoid tissue pool to nonlymphoid tissues would not contribute to lymphocyte homeostasis and therefore would not likely affect our results. In addition, in studies using Thy1.1/1.2 congenic mice, we found that during the one week period of the studies described, all of the adoptively transferred cells could be found within the population with detectable CFSE fluorescence (not shown). That is, we also did not appear to miss cells due to any loss of CFSE label during the brief period of the study. Therefore, in the rest of this report, we combine "cell death" and "migration" together, and refer to it as "cell death".

To sum, among the many potential factors influencing the fates of cells, we have attempted a fairly simplified approach that considers only proliferation potential and cell death as the most important ones to include in our analysis. That is, at any given time point (or within a "cycle") there are only a few fates for a cell at each division: it could survive without further dividing, it could die, or it could divide into the next generation of cells. One complication we consider is possible change in parameters at each successive division to account for progressive differentiation or loss in viability.

We thus assigned the parameters "x" (proportion of dividing cells) and "y" (proportion of dying cells) to represent the "proliferation potential" and "cell death", respectively, for cells in each peak of the CFSE profile. We assume that after each cell division, a peak in the CFSE profile is the result of the summation of existing cells, cells that have entered by cell division from the previous peak, cells lost by death, and cells lost from cell division and entry into the next peak. This can be expressed by an equation: $P_{mn} = P_{m(n-1)} - x_m P_{m(n-1)} - y_m P_{m(n-1)} + 2x_{(m-1)} P_{(m-1)(n-1)}$. In this equation, "m" represents the number of peaks that can be seen in CFSE profile, and "n" represents the hypothetical cell division number. Although these cell populations have not been synchronized *in vivo* or *in vitro*, and there may also be variations in the cell cycling time, we found empirically that using an arbitrary eight cycles during the three-day *in vitro* stimulation or the first seven-day *in vivo* homeostatic proliferation provided for the best fit to the experimental data. For the first peak (m=1), the equation should be expressed as $P_n = P_{n-1} - xP_{n-1} - yP_{n-1}$. As the x and/or y values may not remain the same throughout the proliferation process, "increments" in x and y were considered in the progression from peak to peak. We then generated a matrix of simulated CFSE data given all possible x and y values,

with limited incremental changes at successive cycles for each parameter. This "look up table" was then compared to actual CFSE data to find the parameters most closely fitting the actual peak data. The fit between each of our matrix simulations and the experimental data was estimated using a modified Chi-Square (χ^2) test calcuating the sum of the squared differences in each peak ($\chi^2=\Sigma[P_{mn\ model} - P_{mn\ data}]^2$). A smaller χ^2 value indicates a better fit to the experimental data. We then chose the best fit model among all possible x and y values (with the restriction that the sum of x and y is less than 1) and potential increments in each, against all of our specific sets of experimental CFSE data.

Quantitation of CFSE profiles and mathematical simulation: testing against experimental data

We first tested this system under the more precisely controlled *in vitro* stimulation conditions using anti-CD3 or anti-CD3/CD28. We found that the our mathematical simulation recapitulated the patterns of CFSE dilution profile very closely (Figure 2A). Interestingly, we saw dramatic difference among anti-CD3 alone stimulated, anti-CD3 plus anti-CD28 costimulated proliferation. For instance, for $CD4^+$ T cells, upon anti-CD3 alone stimulation, the initial x was 0.03 with increment of 0.11 and the y was 0.08 with no increment. In contrast, upon anti-CD3 plus anti-CD28 costimulation, the initial x was 0.26, much higher than from anti-CD3 alone stimulation, but with no increment; the y was 0.06, smaller than from anti-CD3 alone stimulation, but with an increment of 0.005. These results indicate that upon anti-CD3 plus anti-CD28 costimulation, a much larger percentage of T cells were to enter cell cycle for the first division, with a similarly high fraction of each subsequent population induced to divide in each successive cycle; in contrast, upon anti-CD3 alone stimulation, only a minor proportion of T cells managed even to make the first division. This would appear to be consistent with our current understanding of the function of CD28 costimulation [16, 17, 19, 28]; interestingly, it also emphasizes the point that not all cells will enter division together even in the presence of a robust anti-CD3 plus anti-CD28 combination. Thus, while a high proportion of cells is ultimately able to divide during the three days, it is not coordinated or else we would only see a single CFSE positive peak move through each cell division, and indeed we recognize a pattern with several peaks as indicative of continuing active cell division among all peak populations.

The results showed a rapid increase in the x parameter for anti-CD3 alone stimulated T cells. This appears to reflect that the very small number of cells able to initiate the first division were more inclined to continue to divide persistently through several cycles. However, considering a higher estimated starting y value (proportion of dying cells) for the anti-CD3 alone stimulated cells, the combination of x and y parameters would still predict a much higher accumulation of proliferating $CD4^+$ T cells induced by anti-CD3/CD28 than by anti-CD3 alone stimulation, consistent with the expected biological consequences of CD28 costimulation.

All calculated parameters were summarized in Figure 2B. From the results, we can see dramatic differences in T cell proliferation behavior between the $CD4^+$ and $CD8^+$ subsets. Furthermore, the results show clear difference in T cell proliferation behavior under different conditions, namely, CD3 stimulation and CD3 plus CD28 costimulation. Therefore, this system is able to simulate the behavior of proliferating T cells.

Differential behaviors of $CD4^+$ and $CD8^+$ T cells in homeostatic proliferation

The CFSE profiles from homeostatically proliferating $CD4^+$ and $CD8^+$ T cells would suggest a faster accumulation of $CD8^+$ T cells in the periphery (Figure 1A). Interestingly, however, seven and fourteen days after transfer, the $CD4^+$ *vs* $CD8^+$ ratios of recovered donor cells were not dramatically changed (Figure 3A). These data suggest that factors regulating homeostatic proliferation may also influence the ratio of the two major T cell sub-populations, even under lymphopenic conditions where the proliferation rates are not equal. It is also possible (though

less likely) that since cross-inhibition of homeostatic proliferation has been reported [4] between lymphocyte subsets, the maintenance of the $CD4^+$ *vs* $CD8^+$ ratio is a secondary consequence of cross-inhibition.

Using the modeling system, we then calculated x and y parameters for adoptively transferred $CD4^+$ as well as $CD8^+$ T cells in homeostatic proliferation experiments. Figure 3B shows the result of comparisons of simulation results and a set of experimental data. We found again that the simulated peaks recapitulated the patterns of the CFSE dilution profile very closely (Figure 3B). The starting x value from homeostatic proliferation was always smaller than that from anti-CD3/CD28 stimulated proliferation, while the starting y value was always higher than that from anti-CD3/CD28 stimulated proliferation. This was true for both $CD4^+$ and $CD8^+$ T cells (Figure 2B and 3C). The combination of these parameters predicted a much slower accumulation of homeostatically proliferating T cells than CD3/CD28 stimulated T cells, even when the different time periods (three days *in vitro* versus seven days *in vivo*) are taken into consideration.

Interestingly, there is a striking difference between the parameters identified for $CD4^+$ and $CD8^+$ T cells (Figure 3C). The parameter x for $CD4^+$ T cells was 0.056 with no increment for any peak; the parameter y for $CD4^+$ T cells was 0.164 with an increment of 0.001 for each peak. In other words, in each cell cycle, 5.6% of transferred BALB/c $CD4^+$ T cells proliferated, while 16.4% of the cells died or left lymphoid organs with the death rate increased by 0.001 for each successive cell cycle. In contrast, the parameter x for $CD8^+$ T cells was 0.056 with an increment of 0.078 for each cycle; the parameter y for $CD8^+$ T cells was 0.212 with an increment of 0.012 for each cycle (Figure 2B and Table 1). Thus, while $CD8^+$ T cells would begin with a similar rate of entry into cycle as $CD4^+$ T cells, the proportion of cells entering cycle would increase after each division. Moreover, though $CD8^+$ cells would be proliferating at a higher rate than $CD4^+$ cells, they also would be entering apoptosis at a higher rate, with increasing apoptosis with each cell division.

These quantitative estimates (x and y factors) confirm the conclusion from direct observation of CFSE data that, compared to $CD4^+$ T cells, the $CD8^+$ T cells proliferated at more rapid rates. In addition, both the proliferation rate and the cell death rate for $CD8^+$ T cells were expected to increase after each successive cell division. For $CD4^+$ T cells, the model predicted that the proliferation rate remains the same, while the cell death rate increases slightly on each successive cell division. Thus, the $CD8^+$ T cells proliferate more rapidly than the $CD4^+$ T cells, but they also die more rapidly than the $CD4^+$ T cells. This may be an important explanation for why $CD8^+$ T cells appeared to proliferate faster based on visual inspection of CFSE data without actually affecting their accumulation and the actual $CD4^+$ *vs* $CD8^+$ ratio. That is, the increasing probabilities of both proliferation and cell death in combination appear to actually prevent the accumulation of dividing cells. The latter conclusion is consistent with previous published data showing that homeostatic proliferation can not fill a lymphopenic environment with a normal number of T cells [29].

Increasing potentials of proliferation and cell death as cells divide

As mentioned earlier, the modeling system predicts that the proportion of cells undergoing apoptosis increases with each successive division, and that, at least for $CD8^+$ T cells, the proportion of cells entering cell cycle also increases with each division. To test these, we performed brief bromodeoxiuridine (BrdU) labeling to detect cells that enter cell cycle and AnnexinV staining to detect apoptotic cells. As shown in Figure 4A, the incorporation of BrdU in non-divided transferred $CD8^+$ T cells (Peak 1) was barely detectable by flow cytometry. Interestingly, percentages of BrdU positive cells increased as transferred cells divided further (Peak2 through Peak6, Figure 4A). These data demonstrate that the proportion of $CD8^+$ T cells entering cell cycle did indeed increase with each successive cell division. Similarly, for

AnnexinV staining on $CD8^+$ T cells, the percentage of AnnexinV positive cells increased as transferred cells divided further (Peak 1 through Peak 6, Figure 4B). These data demonstrate that the proportion of $CD8^+$ T cells undergoing apoptosis increases with each successive cell division. When analyzing transferred $CD4^+$ T cells, we found similar trends on AnnexinV staining positive cells, consistent with the model prediction (data not shown), though the trends were not as striking as reported for superantigen-induced proliferation and apoptosis [18]. We also found that BrdU incorporation of transferred $CD4^+$ T cells displayed a similar trend with that of transferred $CD8^+$ T cells (data not shown). However, for the CD4 T cells, this mismatch between predicted x (with no increment) and BrdU staining (with increasing percentages of BrdU positive cells) may result from the relatively small number of peaks from $CD4^+$ CFSE profiles that hampered an accurate calculation. Additionally, it should be noted that both the short-term BrdU labeling served only as a "snapshot" of the status of the transferred T cells during the period of labeling. Similarly, the percentage of AnnexinV positive cells will be an underestimate due to rapid phagocytosis of apoptotic cells in vivo. Therefore, the percentages of BrdU positive and AnnexinV positive cells should not be expected to exactly match model x and y values, as they can only confirm the trends.

Genetic influence on T cell homeostatic proliferation

Using the modeling system, we then compared T cell homeostatic proliferation on different genetic backgrounds. In these experiments, we transferred CFSE labeled total T cells into sub-lethally irradiated syngeneic mice. The mouse strains we analyzed included BALB/c, C57BL/6 (B6), CB6F1 and NOD. At day seven and day fourteen, we analyzed cells recovered from lymph nodes and spleens. As summarized in Table 1, for all the strains examined, the total T cell recovery (labeled and non-labeled) from irradiated and transferred (Irr) mice was not significantly different than that from irradiated but not transferred (Irr-N) mice. This was true for all strains under evaluation, at both day seven and day fourteen time points (Table 2). These data suggest that even two weeks after transfer, adoptively transferred T cells had not appreciably accumulated via homeostatic proliferation. Consistent with data from BALB/c presented above, the striking differential behavior between $CD4^+$ and $CD8^+$ subsets exists in all tested strains. Moreover, the $CD4^+$ *vs* $CD8^+$ ratios were not significantly changed in proliferating cells from all the strains at all time points.

Interestingly, the CFSE dilution profiles showed different patterns among the strains tested (Figure 5A). For $CD4^+$ T cells, more cells stopped after one division from B6 and CB6F1 mice than from BALB/c mice. In addition, much fewer $CD4^+$ T cells from B6 and CB6F1 mice had gone through second round of division than cells from BALB/c mice. $CD4^+$ T cells from NOD mice displayed a phenotype somewhere in between BALB/c and B6. Similarly, for $CD8^+$ T cells, more cells stopped after one division from B6 and CB6F1 mice; fewer cells from B6, CB6F1 and NOD mice had gone through fifth division than cells from BALB/c mice. These results suggest that the genetic background influences the kinetics of T cell homeostatic proliferation.

Next, we calculated x and y parameters and their increments with the modeling program. Within each strain, the parameters for $CD4^+$ T cells are consistently different from those of $CD8^+$ T cells, with higher x and y values for CD8 T cells (Figure 5B and Table 2). Importantly, the parameters calculated for each strain are all distinct from each other (Figure 4B and Table 1). In the case of $CD4^+$ T cells, cells from BALB/c mice had the highest x values from all the strains tested (5.6%), while $CD4^+$ T cells from B6 mice had the lowest (4%) x values, indicating that $CD4^+$ T cells from BALB/c mice had highest proliferation potential among all the strains under study. However, the differences among x values for $CD4^+$ T cells were not dramatic in general (ranging from 4% to 5.6%). There was no increment with each division for any of the $CD4^+$ T cell x values. When analyzing y values, we observed that $CD4^+$ T cells from B6 mice

had the highest (26%) and cells from NOD mice had the lowest (11%) among all the strains studied. Except for $CD4^+$ T cells from BALB/c mice, which had a minimal y increment (0.001), there was no detectable y increment in $CD4^+$ T cells from any of the other strains. In the case of $CD8^+$ T cells, BALB/c cells had the highest x increment (7.8%) and B6 cells had the lowest x increment (2.3%), similar to NOD $CD8^+$ T cells (3%). Finally, $CD8^+$ T cells from NOD mice had the highest y increment (6.2%) and BALB/c cells had the lowest (1.2%). Interestingly, while $CD4^+$ T cells from CB6F1 mice had an x value (4.3%) very similar to B6, their $CD8^+$ T cells proliferated more like BALB/c $CD8^+$ T cells (Figure 5B and Table 2). Taken together, the combination of x and y values and their respective increments can be viewed as a quantitative characteristic for homeostatic proliferation of certain T cell subsets (*i.e.* $CD4^+$ or $CD8^+$) from certain genetic backgrounds.

To further compare T cell behavior under lymphopenic conditions, we simulated "model peaks" for $CD4^+$ and $CD8^+$ T cells of all the strains using calculated x, y and their increment values (not shown). Then the model peak values were compared pairwise among the strains using χ^2 calculation: $\chi^2=\Sigma[P_{m\ StrainA} - P_{m\ StrainB}]^2$. Here, a smaller χ^2 value indicates a higher similarity among the behaviors of T cells from the two strains. The comparison results are summarized in Table 3. For the $CD4^+$ subset, cells from B6, CB6F1 and NOD mice behaved similarly, while cells from B6 and BALB/c behaved the most differently. For the $CD8^+$ subset, cells from BALB/c mice behaved similarly to cells from CB6F1 mice, which were very different from B6 $CD8^+$ T cells (Table 3).

It should be noted that all the results described above were based on day seven data. If day fourteen data are used to calculate the parameters, all x values, except for those of BALB/c $CD4^+$ T cells, decreased compared to those from day seven data. However, the y values obtained from day fourteen data remain similar to those from day seven data in general. The patterns among all the strains remained very similar. These results suggest that homeostatic proliferation does not proceed linearly, but that it slows down as time passes. Possible factors that could slow down the proliferation of transferred cells may include intrinsic limitations to homeostatic proliferation potential, or the accumulation of thymic emigrants, which may compete with transferred cells for survival factors. It seems likely that the slowed proliferation rate also contributed to the fact that homeostatic proliferation of transferred T cells could not fully repopulate the T cell compartment in lymphopenic individuals.

Discussion

In these studies, we have shown that homeostatic proliferation of T cells can be mathematically quantified for purposes of making comparisons among cell subsets, experimental conditions, and genetic backgrounds. This system was based on assumptions predicting possible fates of transferred T cells, namely the combination of proliferating/non-proliferating, surviving/dying, and migrating/non-migrating. It has been shown that naïve T cells are able to migrate into peripheral non-lymphoid organs [30]. However, we found no appreciable difference in the migration of transferred T cells, compared to those in non-irradiated mice. Thus, we reasoned that the major factors affecting the accumulation of transferred cells would be proliferation potential and survival. By determining x, y and their respective increments, this modeling system provides measurable parameters to T cell homeostatic proliferation. Therefore, studying the effects of certain factor(s) on T cell homeostatic proliferation could be approached as the investigation of how these factors influence the parameters x and y. Moreover, this system assigns quantitative characteristics to certain T cell subsets from certain genetic background. Furthermore, the modeling results revealed measurable differences in the behavior of $CD4^+$ *vs* $CD8^+$ T cell subsets, regardless of conditions and genetic backgrounds. This seems to accurately reflect the differential biology of the two T cell subsets.

There are, however, limitations to this (or any) modeling system. One is that it depends on the detection and resolution of CFSE dilution in proliferating cells. Thus this system would potentially lose track of the rapid "spontaneous proliferation" of a small proportion of T cells transferred into *Rag* deficient or *Cd3ε* deficient mice [29,31–34]. In addition, homeostatic proliferation of T cells does not appear to be consistent over time, as results using the day fourteen data showed slower kinetics than using data from day seven (data not shown). This slowing-down may reflect intrinsic limits to the homeostatic proliferation potential of T lymphocytes [35], changes in the lymphoid stroma that supports the proliferation, or increased competition among lymphocyte populations over time. However, calculations using data from a fixed early time point, such as day seven, did provide a reasonably good basis for comparisons.

When T cells are activated by antigen stimulation, $CD8^+$ T cells proliferate more extensively than $CD4^+$ T cells [36]. Interestingly, in a lymphopenic environment, the antigen independent proliferation of adoptively transferred T cells also shows a similar pattern. When T cells undergo homeostatic proliferation, the $CD4^+$ subset undergo fewer rounds of division than the $CD8^+$ counterpart, a phenomenon that was also previously reported [25,37]. The $CD4^+$ *vs* $CD8^+$ difference in antigen driven proliferation has been attributed to cell intrinsic differences between the two T cell subsets [36]. This may also be true for the antigen independent homeostatic proliferation of $CD4^+$ *vs* $CD8^+$ T cells. For instance, we previously reported evidence that the homeostatic proliferation of $CD4^+$ T cells requires signaling by CCR7 ligands whereas proliferation of $CD8^+$ T cells does not [37]. It is intriguing then that the relatively more rapidly expanding $CD8^+$ T cells do not accumulate at a rate that dramatically changes the $CD4^+$ *vs* $CD8^+$ ratio. It was striking that proliferating $CD8^+$ T cells appeared to be dying more rapidly than their $CD4^+$ counterparts. Our results confirmed this for all mouse strains examined; both parameters x (the proportion of dividing cells entering) and y (the proportion of dying cells) were much higher for $CD8^+$ T cells than for $CD4^+$ T cells. This contradicts the results from a previously published report in which the authors concluded that $CD8^+$ T cells survived better than $CD4^+$ T cells [26]. These differences might be explained by the different experimental systems utilized in the two sets of studies. In the studies reported by Ferreira *et al*, $CD4^+$ or $CD8^+$ TCR transgenic T cells were transferred into *Rag* deficient mice [26]. Thus, their study was essentially focused on comparing different TCR clones. In the studies we reported here, polyclonal T cells from normal wild type mice were transferred with unmodified natural $CD4^+$ *vs* $CD8^+$ ratios, avoiding the introduction of non-physiological competition between the two T cell subpopulations and/or competition among clones in the repertoire [4, 38–41]. Thus, study of T cell homeostatic proliferation of populations instead of clones may represent a more physiological situation. Indeed, it has been shown that polyclonal $CD4^+$ T cells survive longer than $CD8^+$ T cells in the absence of the interaction with MHC class II or MHC class I molecules, respectively [42–44]. Clearly, more work needs to be done to dissect the mechanisms by which the $CD4^+$ *vs* $CD8^+$ ratio is maintained.

In addition to the differential behavior between $CD4^+$ and $CD8^+$ T cells, our analysis system also identified some differences in homeostatic proliferation of T cells from different strains. This suggests that genetic factors also influence T cell homeostatic proliferation, though it is not clear whether these observations point to significant physiological effects on immunity in vivo. Yet it is interesting that many aspects of T cell biology are influenced by genetic backgrounds. For instance, the $CD4^+$ *vs* $CD8^+$ ratio has been demonstrated to vary depending on different mouse strains and has been mapped to several distinct loci including the *Tcrα* locus [45–48]. This may also be true for human [49]. We do not know which loci regulate T cell homeostatic proliferation, but it is likely that multiple loci may be involved, because while $CD4^+$ T cells from CB6F1 mice behaved similarly to those from B6 mice, $CD8^+$ T cells from CB6F1 mice instead behaved similarly to those from BALB/c mice (Figure 4B). Moreover, these studies cannot unequivocally establish whether the genetic differences are cell autonomous or due to effects on stromal cell or dendritic cell contributions to homeostatic

proliferation. Since lymphopenia and T cell homeostatic proliferation are involved in induction and/or precipitation of autoimmune diseases, mapping the loci that influence T cell homeostatic proliferation could provide important insights in the etiology and/or therapies of these diseases. Since our modeling system makes quantitation of this phenomenon possible, it could help the mapping process by defining an inheritable quantitative trait.

Our model shows that, at least for $CD8^+$ T cells, both the proportion of cells that are dividing (x) and the proportion of cells that are dying (y) increase with each cell division, which has been confirmed by short-term BrdU incorporation experiment and by AnnexinV staining of apoptotic cells. Even for the $CD4^+$ T cells that did not have increments in their x and y values, the y values are still relative higher than x values (Figure 4B). These results would lead to an unexpected but important prediction that with the proceeding of cell divisions the combination of the two factors and their increments would not allow the accumulation of proliferating cells. Indeed, the numbers of transferred cells have not increased in two weeks after transfer (Table 2). It has been reported that even months after transfer, the proliferation of transferred T cells could not restore the T cell compartment of T cell depleted recipients [35, 50]. Furthermore, the accumulation of transferred cells in other reports was largely the result of transferred hematopoietic stem cells that contaminated the T cell preparations [35, 51]. Taken together, our results provide a compelling explanation for the observations that homeostatic proliferation of (transferred) T cells are not able to restore the full complement of T lymphocytes in T cell depleted animals. In other words, re-establishing a full T cell population would be a “mission impossible” for transferred T cells.

Homeostatic proliferation has been shown to be able to drive cohorts of transferred T cells to differentiate into memory-like cells [6,9,10,50,52]. These phenotypically converted cells may have survival advantages over others, and would be better able to accumulate in the body. These cells could also be selected by this process for higher affinity against self antigens [53–55]. Thus, lymphopenia and homeostatic proliferation would provide strong predisposing conditions for the induction or precipitation of autoimmune diseases [11,12,13]. In addition to autoimmune diseases, T cell homeostatic proliferation has recently been implicated in more clinical situations, including tolerance induction for organ transplantation, tumor immunotherapy using adoptive transfer of effector T cells [56–60]. All these highlight the importance in elucidating the mechanisms regulating T cell homeostatic proliferation. The studies we reported herein provide a new tool in this field as well as insights to the genetic influence on the phenomenon.

Materials and Methods

Mice

BALB/c, C57BL/6 (B6), F1 of BALB/c × B6 cross (CB6F1), and non-obese diabetic (NOD) mouse strains were purchased from the Jackson Laboratory (Bar Harbor, ME). All mice were housed in a specific pathogen free (SPF) facility at the La Jolla Institute for Allergy and Immunology (LIAI), and the University of California Riverside, and were used at ages ranging 6–10 weeks. Usage of mice was in accordance with institutional IACUC regulations.

T cell purification and labeling

Single cell suspensions were prepared from lymph nodes (LN). Total T cells were purified by depleting cells from other lineages with magnetic micro-beads and Auto-MACS in accordance with manufacturer’s instruction (Miltenyi Biotec Inc, Auburn, CA). This purification method typically yields >97% $CD3^+$ cells. Purified T cells were then labeled with carboxy-fluoresceindiacetate succinimidylester (CFSE) (Invitrogen, Carlsbad, CA). Briefly, purified T cells were resuspended in PBS containing 0.1% BSA; CFSE was then added to cell suspension

to a final concentration of 7.5μM. After incubation at 37° for 15 min, the cells were then washed extensively with RPMI medium.

Irradiation and adoptive transfer

One day before transfer, mice were irradiated at a dose of 500rad. Ten million CFSE labeled T cells were injected *i.v.* into the irradiated mice, with cells injected into recipients of the same strain. Injected mice were then kept in the SPF facility for seven or fourteen days before the analysis. For bromodeoxyuridine (BrdU) incorporation experiments, one day before analysis, mice were injected *i.p.* with BrdU at a dose of 2mg/mouse.

In vitro stimulation of T cells

Stimulation of T cells with anti-CD3 plus anti-CD28-coated beads has been described elsewhere [27]. Briefly, surfactant-free 4.9-μm white polystyrene latex beads (Interfacial Dynamics) were coated with 0.3μg/ml anti-CD3 (145-2C11; BD Pharmingen) with or without 2.7μg/ml anti-CD28 (37.51; eBioscience) in PBS. A hamster IgG isotype control (eBioscience) was used to make the total protein concentration of 5μg/ml. Purified and CFSE loaded total T cells were cultured with equal number of antibody-coated beads for three days.

Flow cytometry

Total LN cells and spleen cells were recovered from adoptively transferred mice and stained with fluorochrome-labeled antibodies. FACS data were collected on a FACScalibur with CellQuest Pro software (BD Bioscience, San Jose, CA). Data analysis was performed with FlowJo software (Tree Star, Ashland, OR). Staining antibodies were purchased from BD Biosciences including PE-Cy5 anti-CD8, PE anti-CD4, APC anti-CD4, PE AnnexinV. To detect BrdU incorporation, a BrdU Flow Kit was used according to manufacturer's instructions (BD Biosciences, San Diego, CA).

Modeling

To describe T cell homeostatic proliferation in a quantitative way, a mathematical simulation was created. The assumption of this method was that the possible fates of adoptively transferred T cells should include surviving but not dying, entry or exit into each peak by dividing, dying, or migrating to peripheral tissues. Thus, after each cell cycle, a peak in CFSE profile should be the result of the combination of cells that have divided from the previous peak, cells that have died, cells that have divided into the next peak, and cells that have migrated to peripheral non-lymphoid organs. This can be expressed by an equation: $P_{mn} = P_{m(n-1)} - x_m P_{m(n-1)} - y_m P_{m(n-1)} + 2x_{(m-1)} P_{(m-1)(n-1)}$. In this equation, for each peak, x was assigned as the parameter for proportion of cells that divide, y was assigned as the parameter for proportion of cells that die or migrate to peripheral tissues, m is the number of peaks that can be found in the CFSE profile, and n in the hypothetical cell cycle number. For the first peak (m=1), the equation should be expressed as $P_n = P_{n-1} - xP_{n-1} - yP_{n-1}$. To compare our model with the experimental data, a modified Chi-Square (χ^2) test was used, by taking the sum of the squared differences in each peak ($\chi^2 = \Sigma[P_{mn\ model} - P_{mn\ data}]^2$). A smaller χ^2 value indicates a better fit of the model to the experimental data. The experimental data were then run in a Java based program written in house, which subsequently creates a matrix of χ^2 values for all possible x, y combinations and possible x and y increments with each cycle. The values of x and y were set ranging from 0.00 to 1.00, with a step of 0.01 and following the rule that the sum of x and y values in a given equation should not be greater than 1.00. Considering that x and y may change from one peak to the next, increments in x and/or y values were allowed ranging from 0.00 to 1.00 with a step of 0.005. This program selects the lowest χ^2 value and its associated parameters to find the best fit to the experimental data. In cases where multiple parameter conditions yield the same χ^2 value, parameters were selected based on the best fit to other replicates in the same experiment.

Averages of x, y and their increments on x and y were calculated from five replicates for each mouse strain.

Acknowledgement

The authors would like to thank Sandy Ngo for technical assistance and Dr. Marta Lopez Fraga for critical reading of the manuscript. This work was supported by the National Institutes of Health (Grant AI63426 to D.D.Lo).

References

1. Almeida AR, Rocha B, Freitas AA, Tanchot C. Homeostasis of T cell numbers: from thymus production to peripheral compartmentalization and the indexation of regulatory T cells. Semin Immunol 2005;17:239–249. [PubMed: 15826829]
2. Jameson SC. T cell homeostasis: keeping useful T cells alive and live T cells useful. Semin Immunol 2005;17:231–237. [PubMed: 15826828]
3. Viret C, Wong FS, Janeway CA Jr. Designing and maintaining the mature TCR repertoire: the continuum of self-peptide:self-MHC complex recognition. Immunity 1999;10:559–568. [PubMed: 10367901]
4. Ernst B, Lee DS, Chang JM, Sprent J, Surh CD. The peptide ligands mediating positive selection in the thymus control T cell survival and homeostatic proliferation in the periphery. Immunity 1999;11:173–181. [PubMed: 10485652]
5. Goldrath AW, Bevan MJ. Low-affinity ligands for the TCR drive proliferation of mature CD8+ T cells in lymphopenic hosts. Immunity 1999;11:183–190. [PubMed: 10485653]
6. Kieper WC, Jameson SC. Homeostatic expansion and phenotypic conversion of naive T cells in response to self peptide/MHC ligands. Proc Natl Acad Sci U S A 1999;96:13306–13311. [PubMed: 10557316]
7. Tan JT, Dudl E, LeRoy E, Murray R, Sprent J, Weinberg KI, Surh CD. IL-7 is critical for homeostatic proliferation and survival of naive T cells. Proc Natl Acad Sci U S A 2001;98:8732–8737. [PubMed: 11447288]
8. Schluns KS, Kieper WC, Jameson SC, Lefrancois L. Interleukin-7 mediates the homeostasis of naive and memory CD8 T cells in vivo. Nat Immunol 2000;1:426–432. [PubMed: 11062503]
9. Cho BK, Rao VP, Ge Q, Eisen HN, Chen J. Homeostasis-stimulated proliferation drives naive T cells to differentiate directly into memory T cells. J Exp Med 2000;192:549–556. [PubMed: 10952724]
10. Oehen S, Brduscha-Riem K. Naive cytotoxic T lymphocytes spontaneously acquire effector function in lymphocytopenic recipients: A pitfall for T cell memory studies? Eur J Immunol 1999;29:608–614. [PubMed: 10064077]
11. Marleau AM, Sarvetnick N. T cell homeostasis in tolerance and immunity. J Leukoc Biol 2005;78:575–584. [PubMed: 15894586]
12. Khoruts A, Fraser JM. A causal link between lymphopenia and autoimmunity. Immunol Lett 2005;98:23–31. [PubMed: 15790505]
13. Baccala R, Theofilopoulos AN. The new paradigm of T-cell homeostatic proliferation-induced autoimmunity. Trends Immunol 2005;26:5–8. [PubMed: 15629402]
14. Jameson SC. Maintaining the norm: T-cell homeostasis. Nat Rev Immunol 2002;2:547–556. [PubMed: 12154374]
15. Surh CD, Sprent J. Regulation of mature T cell homeostasis. Semin Immunol 2005;17:183–191. [PubMed: 15826823]
16. Wells AD, Gudmunsdottir H, Turka LA. Following the fate of individual T cells throughout activation and clonal expansion. J Clin Invest 1997;100:3173–3183. [PubMed: 9399965]
17. Gudmundsdottir H, Wells AD, Turka LA. Dynamics and requirements of T cell clonal expansion in vivo at the single-cell level: effector function is linked to proliferative capacity. J Immunol 1999;162:5212–5223. [PubMed: 10227995]
18. Renno T, Attinger A, Locatelli S, Bakker T, Vacheron S, MacDonald HR. Cutting Edge: Apoptosis of superantigen-activated T cells occurs preferentially after a discrete number of cell divisions in vivo. J Immunol 1999;162:6312–6315. [PubMed: 10352241]

19. Gett AV, Hodgkin PD. A cellular calculus for signal integration by T cells. Nat Immunol 2000;1:239–244. [PubMed: 10973282]
20. Deenick EK, Gett AV, Hodgkin PD. Stochastic model of T cell proliferation: A calculus revealing IL-2 regulation of precursor frequencies, cell cycle time, and survival. J Immunol 2003;170:4963–4972. [PubMed: 12734339]
21. Leon K, Faro J, Carniero J. A general mathematical framework to model generation structure in a population of asynchronously dividing cells. J Theoret Biol 2004;229:455–476. [PubMed: 15246784]
22. Ganusov VV, Pilyugin SS, deBoer RJ, Murali-Krishna K, Ahmed R, Antia R. Quantifying cell turnover using CFSE data. J Immunol Methods 2005;298:183–200. [PubMed: 15847808]
23. deBoer RJ, Ganusov VV, Milutinovic D, Hodgkin PD, Perelson AS. Estimating lymphocyte division and death rtes from CFSE data. Bull Math Biol 2006;68:1011–1031. [PubMed: 16832737]
24. Luzyanina T, Roose D, Schenkel T, Sester M, Ehl S, Meyerhans A, Bocharov G. Numerical modeling of label-structured cell population growth using CFSE distribution data. Theor Biol Med Modelling 2007;4:26–39.
25. Bender J, Mitchell T, Kappler J, Marrack P. CD4+ T cell division in irradiated mice requires peptides distinct from those responsible for thymic selection. J Exp Med 1999;190:367–374. [PubMed: 10430625]
26. Ferreira C, Barthlott T, Garcia S, Zamoyska R, Stockinger B. Differential survival of naive CD4 and CD8 T cells. J Immunol 2000;165:3689–3694. [PubMed: 11034373]
27. Li, CR.; Berg, LJ. Journal of immunology. 174. Baltimore, Md: 2005. Itk is not essential for CD28 signaling in naive T cells; p. 4475-4479.
28. Keir ME, Sharpe AH. The B7/CD28 costimulatory family in autoimmunity. Immunological reviews 2005;204:128–143. [PubMed: 15790355]
29. Tanchot C, Le Campion A, Leaument S, Dautigny N, Lucas B. Naive CD4(+) lymphocytes convert to anergic or memory-like cells in T cell-deprived recipients. Eur J Immunol 2001;31:2256–2265. [PubMed: 11477537]
30. Cose S, Brammer C, Khanna KM, Masopust D, Lefrancois L. Evidence that a significant number of naive T cells enter non-lymphoid organs as part of a normal migratory pathway. Eur J Immunol 2006;36:1423–1433. [PubMed: 16708400]
31. Min B, Foucras G, Meier-Schellersheim M, Paul WE. Spontaneous proliferation, a response of naive CD4 T cells determined by the diversity of the memory cell repertoire. Proc Natl Acad Sci U S A 2004;101:3874–3879. [PubMed: 15001705]
32. Min B, Yamane H, Hu-Li J, Paul WE. Spontaneous and homeostatic proliferation of CD4 T cells are regulated by different mechanisms. J Immunol 2005;174:6039–6044. [PubMed: 15879097]
33. Martin B, Becourt C, Bienvenu B, Lucas B. Self-recognition is crucial for maintaining the peripheral CD4+ T-cell pool in a nonlymphopenic environment. Blood 2006;108:270–277. [PubMed: 16527889]
34. Min B, Paul WE. Endogenous proliferation: burst-like CD4 T cell proliferation in lymphopenic settings. Semin Immunol 2005;17:201–207. [PubMed: 15826825]
35. Tanchot C, Le Campion A, Martin B, Leaument S, Dautigny N, Lucas B. Conversion of naive T cells to a memory-like phenotype in lymphopenic hosts is not related to a homeostatic mechanism that fills the peripheral naive T cell pool. J Immunol 2002;168:5042–5046. [PubMed: 11994456]
36. Foulds KE, Zenewicz LA, Shedlock DJ, Jiang J, Troy AE, Shen H. Cutting edge: CD4 and CD8 T cells are intrinsically different in their proliferative responses. J Immunol 2002;168:1528–1532. [PubMed: 11823476]
37. Ploix, C.; Lo, D.; Carson, MJ. Journal of immunology. 167. Baltimore, Md: 2001. A ligand for the chemokine receptor CCR7 can influence the homeostatic proliferation of CD4 T cells and progression of autoimmunity; p. 6724-6730.
38. Rocha B, Dautigny N, Pereira P. Peripheral T lymphocytes: expansion potential and homeostatic regulation of pool sizes and CD4/CD8 ratios in vivo. European journal of immunology 1989;19:905–911. [PubMed: 2500349]
39. Freitas AA, Rocha B. Population biology of lymphocytes: the flight for survival. Annu Rev Immunol 2000;18:83–111. [PubMed: 10837053]

40. Troy AE, Shen H. Cutting edge: homeostatic proliferation of peripheral T lymphocytes is regulated by clonal competition. J Immunol 2003;170:672–676. [PubMed: 12517927]
41. Hataye J, Moon JJ, Khoruts A, Reilly C, Jenkins MK. Naive and memory CD4+ T cell survival controlled by clonal abundance. Science 2006;312:114–116. [PubMed: 16513943]
42. Rooke R, Waltzinger C, Benoist C, Mathis D. Targeted complementation of MHC class II deficiency by intrathymic delivery of recombinant adenoviruses. Immunity 1997;7:123–134. [PubMed: 9252125]
43. Takeda S, Rodewald HR, Arakawa H, Bluethmann H, Shimizu T. MHC class II molecules are not required for survival of newly generated CD4+ T cells, but affect their long-term life span. Immunity 1996;5:217–228. [PubMed: 8808677]
44. Nesic, D.; Vukmanovic, S. Journal of immunology. 160. Baltimore, Md: 1998. MHC class I is required for peripheral accumulation of CD8+ thymic emigrants; p. 3705-3712.
45. Kraal G, Weissman IL, Butcher EC. Genetic control of T-cell subset representation in inbred mice. Immunogenetics 1983;18:585–592. [PubMed: 6606619]
46. Sprent J, Schaefer M. Antigen-presenting cells for unprimed T cells. Immunology today 1989;10:17–23. [PubMed: 2526637]
47. Sim BC, Aftahi N, Reilly C, Bogen B, Schwartz RH, Gascoigne NR, Lo D. Thymic skewing of the CD4/CD8 ratio maps with the T-cell receptor alpha-chain locus. Current biology 1998;8:701–704. [PubMed: 9637921]
48. Myrick C, DiGuisto R, DeWolfe J, Bowen E, Kappler J, Marrack P, Wakeland EK. Linkage analysis of variations in CD4:CD8 T cell subsets between C57BL/6 and DBA/2. Genes and immunity 2002;3:144–150. [PubMed: 12070778]
49. Amadori A, Zamarchi R, De Silvestro G, Forza G, Cavatton G, Danieli GA, Clementi M, Chieco-Bianchi L. Genetic control of the CD4/CD8 T-cell ratio in humans. Nature medicine 1995;1:1279–1283.
50. Goldrath AW, Bogatzki LY, Bevan MJ. Naive T cells transiently acquire a memory-like phenotype during homeostasis-driven proliferation. J Exp Med 2000;192:557–564. [PubMed: 10952725]
51. Ge Q, Hu H, Eisen HN, Chen J. Different contributions of thymopoiesis and homeostasis-driven proliferation to the reconstitution of naive and memory T cell compartments. Proc Natl Acad Sci U S A 2002;99:2989–2994. [PubMed: 11880642]
52. Ge Q, Hu H, Eisen HN, Chen J. Naive to memory T-cell differentiation during homeostasis-driven proliferation. Microbes Infect 2002;4:555–558. [PubMed: 11959511]
53. Ge Q, Rao VP, Cho BK, Eisen HN, Chen J. Dependence of lymphopenia-induced T cell proliferation on the abundance of peptide/ MHC epitopes and strength of their interaction with T cell receptors. Proc Natl Acad Sci U S A 2001;98:1728–1733. [PubMed: 11172019]
54. Moses CT, Thorstenson KM, Jameson SC, Khoruts A. Competition for self ligands restrains homeostatic proliferation of naive CD4 T cells. Proc Natl Acad Sci U S A 2003;100:1185–1190. [PubMed: 12525694]
55. Kieper WC, Burghardt JT, Surh CD. A role for TCR affinity in regulating naive T cell homeostasis. J Immunol 2004;172:40–44. [PubMed: 14688307]
56. Gattinoni L, Finkelstein SE, Klebanoff CA, Antony PA, Palmer DC, Spiess PJ, Hwang LN, Yu Z, Wrzesinski C, Heimann DM, Surh CD, Rosenberg SA, Restifo NP. Removal of homeostatic cytokine sinks by lymphodepletion enhances the efficacy of adoptively transferred tumor-specific CD8+ T cells. J Exp Med 2005;202:907–912. [PubMed: 16203864]
57. Wu Z, Bensinger SJ, Zhang J, Chen C, Yuan X, Huang X, Markmann JF, Kassaee A, Rosengard BR, Hancock WW, Sayegh MH, Turka LA. Homeostatic proliferation is a barrier to transplantation tolerance. Nature medicine 2004;10:87–92.
58. Brown IE, Blank C, Kline J, Kacha AK, Gajewski TF. Homeostatic proliferation as an isolated variable reverses CD8+ T cell anergy and promotes tumor rejection. J Immunol 2006;177:4521–4529. [PubMed: 16982889]
59. Maile R, Barnes CM, Nielsen AI, Meyer AA, Frelinger JA, Cairns BA. Lymphopenia-induced homeostatic proliferation of CD8+ T cells is a mechanism for effective allogeneic skin graft rejection following burn injury. J Immunol 2006;176:6717–6726. [PubMed: 16709831]

60. Khiong K, Murakami M, Kitabayashi C, Ueda N, Sawa SI, Sakamoto A, Kotzin BL, Rozzo SJ, Ishihara K, Verella-Garcia M, Kappler J, Marrack P, Hirano T. Homeostatically proliferating CD4 T cells are involved in the pathogenesis of an Omenn syndrome murine model. 2007;117:1270–1281.

Abbreviations

CFSE, carboxy-fluorescein-diacetate succinimidylester; BrdU, bromodeoxiuridine.

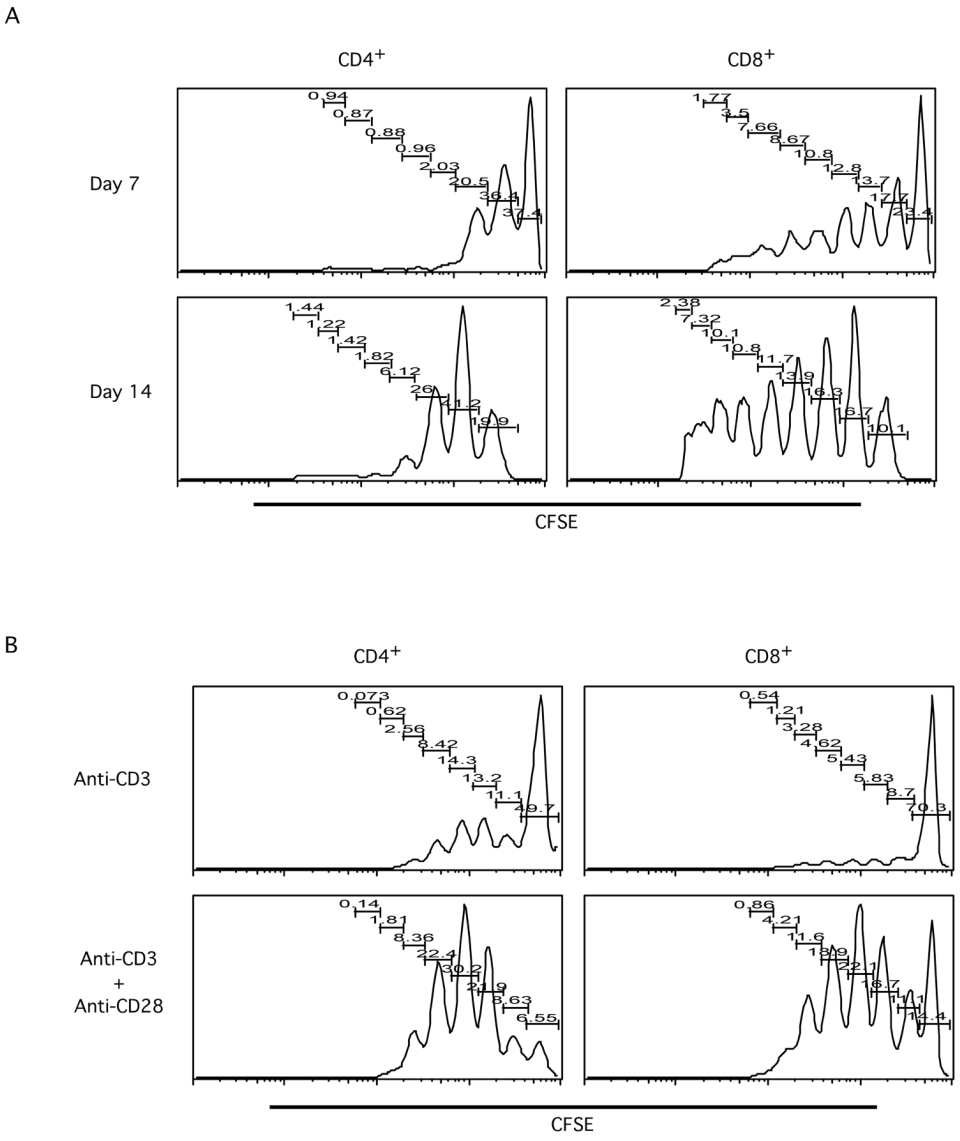

Figure 1. Differential behavior of CD4$^+$ and CD8$^+$ T cells undergoing homeostatic proliferation

Total T cells were purified from lymph nodes (LN) of BALB/c mice by MACS; purified T cells were then labeled with CFSE.

A. Labeled T cells were transferred into sub-lethally irradiated BALB/c mice. Seven and fourteen days later, transferred cells were analyzed by flow cytometry. Histograms show the CFSE profiles of transferred T cells in the CD4$^+$ and CD8$^+$ subsets at day seven and day fourteen time points. Data shown are recovered cells from one representative recipient animal at each time point.

B. Labeled T cells were cultured with anti-CD3 or anti-CD3 plus anti-CD28 coated beads for three days. Cultured cells were then stained for CD4 and CD8, and subjected to FACS analysis. Histograms show CFSE profiles of gated CD4$^+$ or CD8$^+$ cells under different stimulation conditions. Data shown are representatives of three independent experiments.

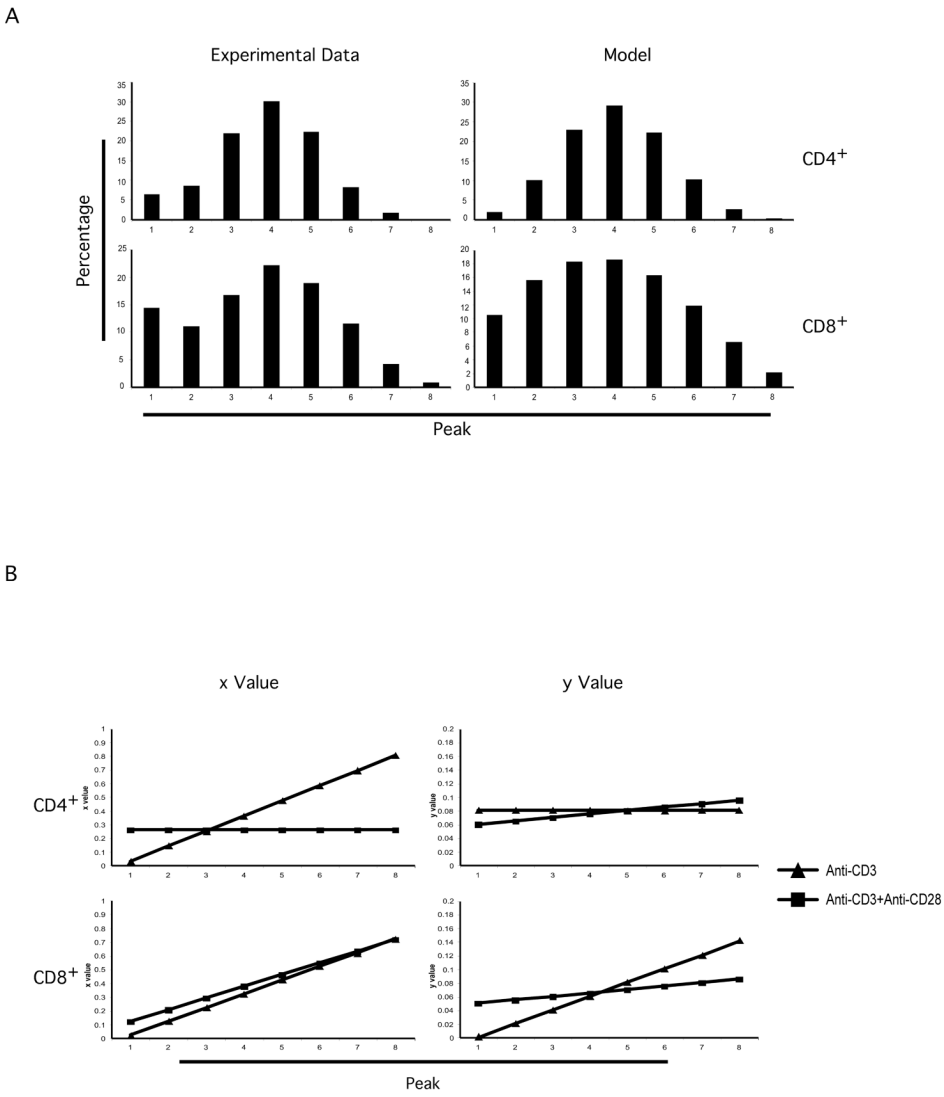

Figure 2. Testing modeling system in *in vitro* T cell activation experiment

T cell purification, labeling and stimulation were performed as in Figure 1B. The percentage of each peak in CFSE profiles was calculated. These numbers were used to calculate the x and y parameters for $CD4^+$ and $CD8^+$ T cells as described in Materials and Methods and in the text.

A. The calculated parameters, x (the proportion of dividing cells) and y (the proportion of dying cells), were used to build models simulating the peaks in CFSE dilution profiles. Graph shows the comparison between experimental data (at left) and model results (at right) from anti-CD3 plus anti-CD28 costimulation experiment.

B. Calculated x (the proportion of dividing cells) and y (the proportion of dying cells) values were graphed, showing dramatic difference anti-CD3 alone stimulation- and anti-CD3 plus anti-CD28 costimulation-induced T cell proliferation within the $CD4^+$ or $CD8^+$ subsets.

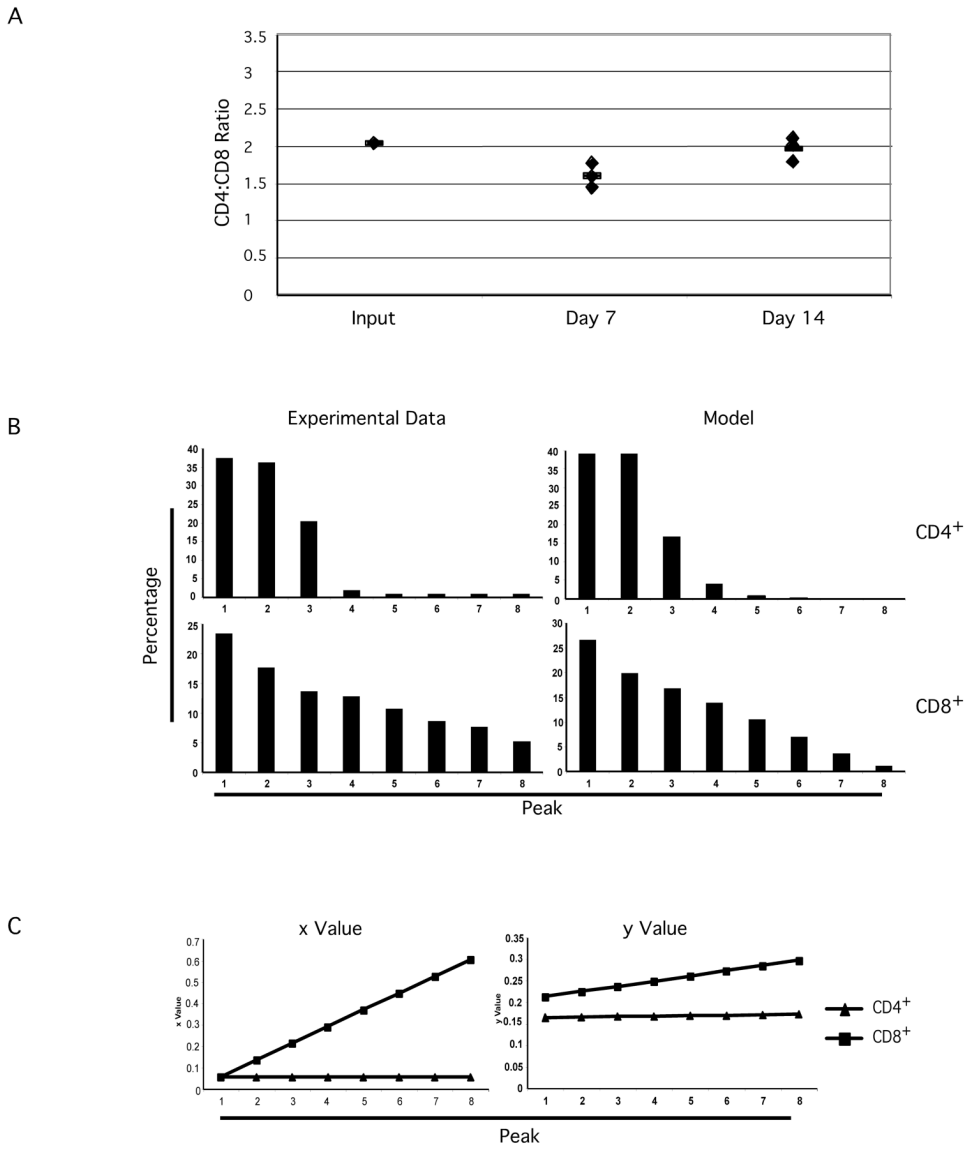

Figure 3. Differential T cell behavior of CD4$^+$ and CD8$^+$ subsets in homeostatic proliferation

T cell purification, CFSE labeling, and adoptive transfer were performed as in Figure 1A.

A. CD4$^+$ *vs* CD8$^+$ ratios were calculated for purified total T cells from BALB/c lymph nodes (Input), recovered CFSE positive T cells at day seven and day fourteen after adoptive transfer, respectively.

B. The percentage of each peak in CFSE profiles was calculated. These numbers were used to calculate the x and y parameters for CD4$^+$ and CD8$^+$ T cells as described in Materials and Methods and in the text. The calculated parameters, x (the proportion of dividing cells) and y (the proportion of dying cells), were used to build models simulating the peaks in CFSE dilution profiles. Graph shows the comparison between experimental data (at left) and model results (at right).

C. The x (the proportion of dividing cells) and y (the proportion of dying cells) parameters were calculated as described in Materials and Methods and in the text. Graphs show the comparisons of x and y parameters for CD4$^+$ and CD8$^+$ T cell subsets under homeostatic proliferation.

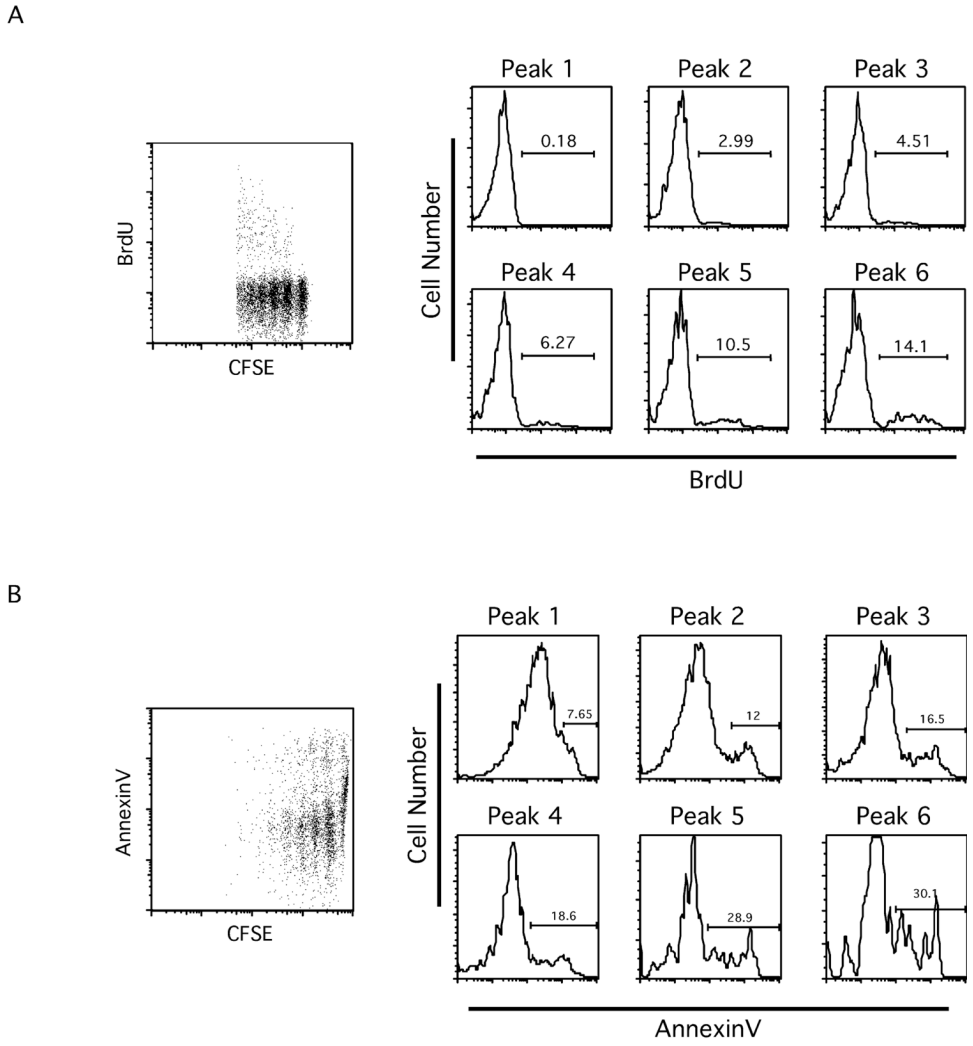

Figure 4. With each successive division, both the proportion of cells entering cell cycle and the proportion of cells undergoing apoptosis increase

T cell purification, labeling and adoptive transfer were performed as in Figure 1A. One day before organ harvest, mice were injected *i.p.* with BrdU (2mg/mouse). BrdU staining (A) and AnnexinV staining (B) were performed as described in Materials and Methods.

A. Dot plot showing BrdU *vs* CFSE profiles from transferred $CD8^+$ T cells. Histograms show BrdU staining for each CFSE peak.

B. Dot plot showing AnnexinV *vs* CFSE profiles from transferred $CD8^+$ T cells. Histograms show AnnexinV staining for each CFSE peak. Data shown are representative of five mice from two experiments.

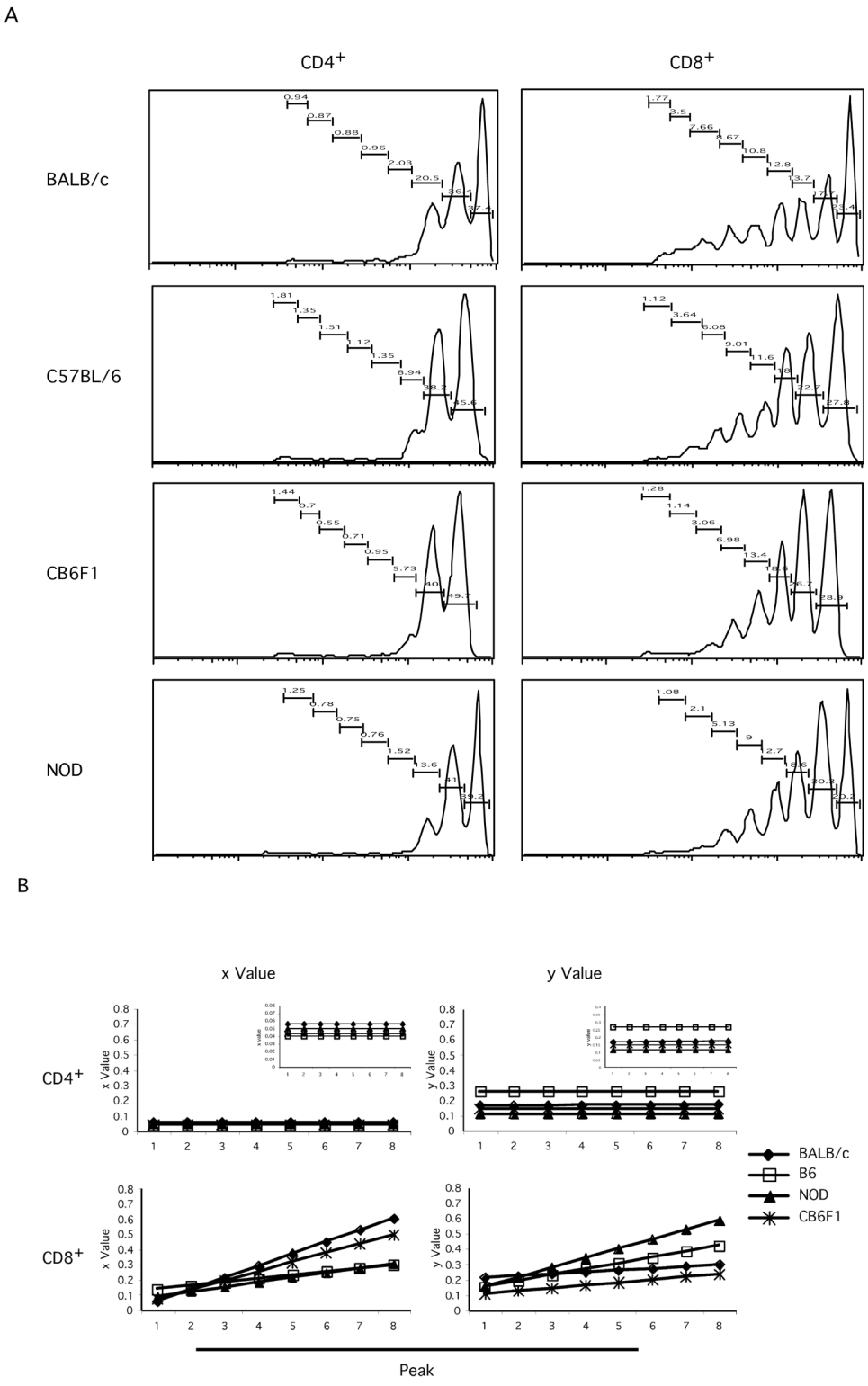

Figure 5. Quantitative modeling analysis reveals differential T cell homeostatic proliferation behavior on different genetic backgrounds

T cell purification, labeling and adoptive transfer were performed as in Figure 1A, but on different mouse strains including BALB/c, B6, CB6F1, and NOD. Seven and fourteen days

later, transferred cells were analyzed by flow cytometry. The x (the proportion of dividing cells) and y (the proportion of dying cells) parameters were calculated for $CD4^+$ and $CD8^+$ T cells from each strain, as described in Methods and text.

A. Histograms show CFSE profiles of transferred T cells in the $CD4^+$ and $CD8^+$ subsets from each strain at day seven time point.

B. Graphs show the comparisons of x (the proportion of dividing cells) and y (the proportion of dying cells) parameters for $CD4^+$ and $CD8^+$ T cell subsets from all strains, respectively. (Insets in the $CD4^+$ panels show same data but on smaller scales.)

Table 1

Calculated parameters from Day 7 and Day 14 transferred cells

a. Day 7

	CD4+				CD8+			
	x	**x Increment**	**y**	**y Increment**	**x**	**x Increment**	**y**	**y Increment**
C57BL/6	0.04	0	0.26	0	0.136	0.023	0.154	0.038
BALB/c	0.056	0	0.164	0.001	0.056	0.078	0.212	0.012
CB6F1	0.043	0	0.143	0	0.073	0.060	0.107	0.018
NOD	0.05	0	0.11	0	0.09	0.030	0.153	0.062

b. Day 14

	CD4+				CD8+			
	x	**x Increment**	**y**	**y Increment**	**x**	**x Increment**	**y**	**y Increment**
C57BL/6	0.025	0	0.63	0	0.065	0.025	0.08	0
BALB/c	0.105	0	0.14	0	0.056	0.032	0.192	0.014
CB6F1	0.037	0	0.5	0	0.043	0.03	0.19	0.0067
NOD	0.043	0	0.5	0	0.05	0.017	0.247	0.025

x: proportion of cells divided

y: proportion of cells died

Data shown are average of 5 mice for each group

Table 2

Cell count of total T cells recovered from LN and Spleen ($x10^5$)

	Normal	Irr-N Day 7	Irr Day 7	Irr-N Day 14	Irr Day 14
C57BL/6	247.8±56.7 (5)	27.4±10.5 (3)	19.7±1.6 (6)	79.2±29.9 (3)	66.6±24.7 (6)
BALB/c	364.8±89.7 (5)	23.3±5.5 (3)	23.3±11.1 (6)	74.1 (1)	65.1±8.1 (6)
CB6F1	234.7±59.6 (3)	15.6 (1)	25.2±3.4 (3)	71 (1)	55.5±2.9 (3)
NOD	295.2±15.4 (3)	ND	48.6±7.78 (3)	ND	54.3±19.6 (3)

Irr: mice that have been irradiated and transferred with T cells

Irr-N: mice that have been irradiated but not transferred with T cells

ND: Not determined

Numbers in the parentheses show the number of mice in each group.

Table 3

Comparison of models among different strains (Chi-square values)

	$CD4^+$	$CD8^+$
BALB/c *vs* B6	80.63	397.57
BALB/c *vs* NOD	54.36	198.32
B6 *vs* NOD	2.6	383.47
BALB/c *vs* CB6F1	137.01	52.73
B6 *vs* CB6F1	7.5	324.97